International Journal of Advanced Research in Electrical, Electronics and Instrumentation Engineering (IJAREEIE)

| e-ISSN: 2278 – 8875, p-ISSN: 2320 – 3765| www.ijareeie.com | Impact Factor: 7.122|

|| Volume 9, Issue 7, July 2020 ||

Observer and Neural Network-Based Fault-Tolerant Nonlinear Controller for Unmanned Surface Vehicle Steering System

Olivier Baraka Mushage

Associate Professor, Faculty of Applied Sciences and Technoogies, Université Libre des pays des Grands Lacs, DRC

ABSTRACT:This paper addresses the control problem of an Unmanned Surface Vehicle steering system subject to unknown dynamics, external disturbances caused by the ship's operating conditions and environment, actuation failure and unavailable state measurement. An adaptive nonlinear controller is developed using Radial Basis Functions Neural Networks, a high-gain state observer and some dynamic parameters such that all the aforementioned challenges are tackled simultaneously. Using the Lyapunov's theory, a stability analysis is performed. In order to illustrate the efficiency of the proposed controller, a MATLAB/SIMULINK simulation is performed with the ships subject to disturbances. The results obtained demonstrate the good tracking behaviour obtained thanks to the proposed controller such that the vessel can perform its missions autonomously despite some adverse conditions.

KEYWORDS: Radial basis function neural network, unmanned surface vehicle, nonlinear control, adaptive control.

I.INTRODUCTION

Unmanned Surface Vehicles (USVs), which are also called Autonomous Surface Crafts or Autonomous Surface Vehicles, are a type of vessel that runs on the surface of water without a pilot on it[1, 2]. Their first use can be tracked back to World War II, where they were used for military purpose. USVs can be used, in a cheaper and safer way, for different missions such as environmental monitoring, defence, scientific studies, general robotic researches, target objects searching, oil spill monitoring and handling, bathymetric mapping, post-disaster search, border patrol,communication relays for Under Water Autonomous Vehicles [1-6]. The great challenge posed by USVs is to improve the automation level in practical application [7].

Changes such as water depth, cruising speed, and ship loading lead to various changes in the USV's dynamics such that the USV is a time varying nonlinear system with parameters uncertainty [8-13]. In addition to these changes, external disturbance like wind, wave, and current make more difficult for the USVs to accomplish their mission. Therefore, the design of efficient controllers for USVs, able to tackle the aforementioned perturbation, is an important task, which has received a tremendous attention from the scientific community.

Considering the fact that USVs are complex nonlinear, time varying and uncertain systems for which precise kinematics model is difficult to obtain and external disturbance effects need to be cancelled, adaptive robust controllers are needed to guarantee USVs' successful accomplishment of their desired mission. Different types of adaptive controllers have been proposed using different approaches. For instance, in [6] an adaptive sliding mode controller (SMC) for a USV's steering system has been developed by using two parallel Radial Basis Function Neural Networks (RBFNNs) for approximating the unknown nonlinear yaw dynamics and for adjusting the control gain (to cancel the effects of external disturbances), respectively. The speed and steering controller design for manoeuvring motions of a UVS was addressed in [7]. An adaptive SMC was designed such that the USV can track a desired velocity and to estimate unknown parameters for the separated surge motion. An augmented model including the heading motion and output tracking error integral was presented and used to design an observer-based model reference adaptive controller.Another adaptive steering control law for a robotic USV was developed in [9] using a predictor, a tracking differentiator, neural networks, and a dynamic surface control technique. The proposed control law was designed to tackle issues related uncertain parameters, time varying disturbances and measurement noises. The heading control problem of an uncertain USVs was addressed in [10] using the model-free adaptive control theory.A robust adaptive autopilot for uninhabited USV based on a model predictivecontroller (MPC) is presented in[12]. The proposed MPC was adaptive thanks to theuse of three algorithms, individually: gradient descent, least squares and weightedleast squares (WLS). In order to overcome the input saturation caused by the limitation of the steering engine of a USV, a feedback control law, based on backstepping design method, was presented in [7]. This feedback control law was used with an auxiliary system to handle the effect of input saturation.

It is clear from the above discussion that there exist in the literature different studies of adaptive controllers able to tackle perturbations like external disturbances, uncertain parameters and actuator saturation. However, only a few of them, to the best of our knowledge, address simultaneously, in addition to the aforementioned disturbances, issues related to unavailable measurements, and actuation faults and saturation.

Motivated by the above discussion, this paper proposes an autopilot based on a nonlinear adaptive control law that can effectively cancel, simultaneously, adverse effects related to time-varying parameters, external disturbances, unavailable measurements, input saturation and actuation faults for a USV, will limited effort. This controller is developed using a high-gain state and RBFNNs.

The remainder of this article is organized as follows.In section II, abrief descriptionof the kinematics model of USV, of the high-gain state observer and of the Radial basis function Neural Network are proposed. In sectionIII, the design ofthe controllerand the stability analysis of the closed-loop system are discussed.Simulations results and discussions are presented in section IV before the paper is concluded in section V.

II.PROBLEM STATEMENT AND PRELIMINARIES

This section presents the control problem of the UVS steering system subject to uncertain dynamics, external disturbances, unavailable measurement and actuation fault. The mathematical model of the UVS steering system is presented as well with some details on the high-gain state observer.

II.1. PRESENTATION OF THE USV MODEL

In this paper we consider the steering system of the marine surface vehicle called DH-01, which is a modified version of a remote-controlled ship[14]. This steering system is characterized by some nonlinearity related to the nonlinear characteristics of fluid force and by some uncertainty in parameters values caused by changes of cruise speed and the external environment. In this paper we discuss the motion control of this ship in the horizontal plane. The motion model in this plane is illustrated in Fig. 1 where $\psi(t)$ is the heading or yaw angle of the USV, while $\delta(t)$ is the rudder angle, which controls the heading.

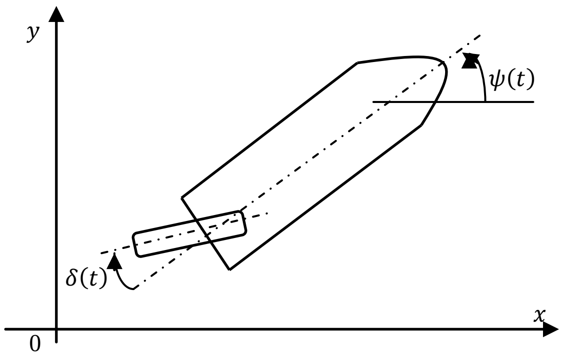

Fig. 1 The motion model of the USV

On the basis of the linear second-order K-T equation, the mathematical model of the USV's steering system is described as follows [8,14,17-19]:

$$\begin{cases} \dot{\psi}(t) = r(t) \\ \dot{r}(t) = -\frac{K(t)}{T(t)}H(r) + \frac{K(t)}{T(t)}\delta(t) + d(t) \end{cases} \tag{1}$$

where $r(t)$ is the yaw angle change rate, $d(t)$ is the external disturbance, $H(r)$ is an uncertain nonlinear function expressed as follows[8]:

$$H(r) = \alpha(t)r(t) + \beta(t)r^3(t) \tag{2}$$

$\alpha(t)$,$\beta(t)$, $K(t)$ and $T(t)$ are coefficients that are positive for a stable movement of the ship, and which are affected by changes in ship's quality, shape, cruise speed, and external environment. It is complicated to find the mathematical relationship between these coefficients with the cruise speed together with the environment, which makes the system controller design challenging such that controllers free of these parameters are needed [8].

Equation (1) can be rewritten as follows:

$$\begin{cases} \dot{x}_1(t) = x_2(t) \\ \dot{x}_2(t) = f(t, x_2) + g(t)u(t) + d(t) \end{cases} \tag{3}$$

where $x_1(t) = \psi(t)$, $x_2(t) = r(t)$, $u(t) = \delta(t)$, $f(t, x_2) = -K(t) \cdot H(x_2)/T(t)$ and $g(t) = K(t)/T(t)$. Knowing that $f(t, x_2)$ is uncertain nonlinear function, and that $g(t)$ varies with the unpredictable cruise speed and external environment, we need to design a controller for which the implementation does not involve these two uncertain functions.

Another issue that can disturb the USV's movement is a rudder failure such as actuator'sloss of effectiveness. Hence, the actuator's output can be expressed as follows [19, 20]:

$$u(t) = (1 - g_a)u_i(t) \tag{4}$$

where $0 \leq g_a < 1$is the degree to which the effectiveness is lost and $u_i(t)$ is the rudder's actuator input.

Let us apply Eq. (4) in Eq. (3) so that we obtain:

$$\dot{x}_2(t) = f(t, x_2) + g(t)u_i(t) + D(t, u_i) \tag{5}$$

where $D(t, u_i) = -g_a \cdot g(t) \cdot u_i(t) + d(t)$ is a lumped disturbance, which is unknown.

The control objective is to make sure that the USV's actuator can generate a rudder angle $u(t)$ that guarantee that the system's yaw angle $x_1(t) = \psi(t)$ can track a given desired value $x_{1d}(t)$ regardless of potential perturbations related to parameters changes, actuation failure and external disturbances. This control must be such that the system's state $\boldsymbol{x} = [x_1, x_2]^T$remains bounded over a compact set $\Omega \subset \mathbb{R}^2$.

Assumption 1: The desired yaw angle $x_{1d}(t)$ is available, continuous and bounded.

Generally, the system's states $x_1(t)$ and $x_2(t)$ are provided to the control system through sensor measurements. However, the effectiveness of the control system can be subject to deterioration caused by malfunctioning sensors. Therefore, a control system with reduced number of sensors is interesting. In this paper, we consider that only yaw angle sensor measurement is available.

In order to deal with uncertain dynamics and unavailable sensor measurements, systems like RBFNN and high-gain state observerare used, respectively.These two systems are presented in the following subsections.

II.2. THE HIGH-GAIN STATE OBSERVER

By considering that only a yaw angle sensor is available to provide a measurement of $x_1(t)$ such that the yaw rate's value $x_2(t)$ needs to be estimated, knowing that the system's dynamics is unavailable, and only the system's output$x_1(t)$ is available, let us use a high-gain state observer modelled as follows[20, 21]:

$$\begin{cases} \dot{\hat{\boldsymbol{x}}} = \boldsymbol{A}\hat{\boldsymbol{x}} + \boldsymbol{L}(x_1 - \hat{x}_1) \\ \hat{y} = \hat{x}_1 \end{cases} \tag{6}$$

where $\hat{\boldsymbol{x}} = [\hat{x}_1, \hat{x}_2]^T$is the estimated state vector,$\boldsymbol{A} = \begin{bmatrix} 0 & 1 \\ 0 & 0 \end{bmatrix}$,$L = [k_1/\epsilon, k_2/\epsilon^2]^T$ is the high-gain vector where $\epsilon > 0$ is a small design parameter; k_1 and k_2 are constant design parameters selected using the pole placement method such that the polynomial :

$$p^2 + k_2 p + k_1 = 0 \tag{7}$$

is Hurwitz stable.

Let us rewrite Eq. (3), where Eq. (5) is used, as follows:

$$\begin{cases} \dot{\boldsymbol{x}} = \boldsymbol{A}\boldsymbol{x} + \boldsymbol{F}(t, x, u_i) \\ y = x_1 \end{cases} \tag{8}$$

where $\boldsymbol{F}(t, x, u_i) = [0 \quad f(t, x_2) + g(t)u_i(t) + D(t, u_i)]^T$.

Remark: During the transient phase, an important offset between the initial value of the yaw angle $x_1(0)$and its desired value $x_{1d}(0)$ can lead to the generation of an important control signal or rudder angle. In order to make sure that this value of rudder angle is restrained between the allowed boundaries, we consider that the actuator's output signal $u \quad (t)$

is bounded in a non-empty set $U \subset \mathbb{R}$. This set is defined as $U \coloneqq \{u \in \mathbb{R}: u_{min} \leq u \ (t) \leq u_{max}\}$ where u_{min} and u_{max} are constraints on the minimum and maximum values of the rudder angle expressed as follows:

$$u(t) = \begin{cases} u_{min} \text{ if } u_a \leq u_{min} \\ u_{max} \text{ if } u_a \geq u_{max} \\ u_a \text{ otherwise} \end{cases} \tag{9}$$

where $u_a\,(t) = (1 - g_a)u_i$.

Assumption 2 [20, 22]: Considering that the state variables x_1 and x_2 are bounded in the compact set $\Omega \subset \mathbb{R}^2$, that the lumped disturbance is $D(t, u_i) \leq \Delta$ and the control signal is $|u(t)| \leq u_{max}$, the nonlinear vector field $\boldsymbol{F}(t, x, u_i)$ is bounded with respect to its arguments on Ω. Hence, there exists a positive value $\Gamma \in \mathbb{R}$ such that $\|\boldsymbol{F}(t, x, u_i)\| \leq \|\boldsymbol{P}\|^{-1}\Gamma \forall \boldsymbol{x} \in \Omega$ with $\boldsymbol{P} = \boldsymbol{P}^T > 0$.

Let us denote $\tilde{\boldsymbol{x}} = \boldsymbol{x} - \hat{\boldsymbol{x}}$as the observation error vector such that its dynamics is obtained as follows:

$$\dot{\tilde{\boldsymbol{x}}} = \boldsymbol{A_0}\tilde{\boldsymbol{x}} + \boldsymbol{F}(t, \boldsymbol{x}, u_i) \tag{10}$$

where $\boldsymbol{A_0} = \boldsymbol{A} - \boldsymbol{L}\boldsymbol{C^T}$ where$\boldsymbol{C^T} = [1 \quad 0]^T$.

Considering assumption 1, let us check the convergence property of the state observer using the following candidate Lyapunov's function:

$$V = \frac{1}{2}\tilde{\boldsymbol{x}}^{\boldsymbol{T}}\boldsymbol{P}\tilde{\boldsymbol{x}} \tag{11}$$

where $\boldsymbol{P} = \boldsymbol{P}^T > 0 \in \mathbb{R}^{2\times 2}$ is a solution to the following Riccati algebraic equation:

$$\boldsymbol{A_0^T P} + \boldsymbol{P A_0} = -\boldsymbol{Q} \tag{12}$$

for a given matrix $\boldsymbol{Q} = \boldsymbol{Q^T} > 0 \in \mathbb{R}^{2\times 2}$.

The fist-time derivative of Eq. (11), where Eq. (12) is used, yields:

$$\dot{V} = \frac{1}{2}\dot{\tilde{\boldsymbol{x}}}^T\boldsymbol{P}\tilde{\boldsymbol{x}} + \frac{1}{2}\tilde{\boldsymbol{x}}^T\boldsymbol{P}\dot{\tilde{\boldsymbol{x}}} = \frac{1}{2}\tilde{\boldsymbol{x}}^T\left(\boldsymbol{A_0^T P} + \boldsymbol{P A_0}\right)\tilde{\boldsymbol{x}} + \tilde{\boldsymbol{x}}^{\boldsymbol{T}}\boldsymbol{P}\boldsymbol{F}(t, \boldsymbol{x}, u_i) = -\frac{1}{2}\tilde{\boldsymbol{x}}^T\boldsymbol{Q}\tilde{\boldsymbol{x}} + \tilde{\boldsymbol{x}}^{\boldsymbol{T}}\boldsymbol{P}\boldsymbol{F}(t, \boldsymbol{x}, u_i) \tag{13}$$

$$\Leftrightarrow \dot{V} \leq -\frac{1}{2}\lambda_{min}(\boldsymbol{Q})\|\tilde{\boldsymbol{x}}\|^2 + \|\tilde{\boldsymbol{x}}\|\|\boldsymbol{P}\|\|\boldsymbol{F}(t, \boldsymbol{x}, u_i)\| \leq -\frac{1}{2}\lambda_{min}(\boldsymbol{Q})\|\tilde{\boldsymbol{x}}\|^2 + \|\tilde{\boldsymbol{x}}\|\Gamma \leq 0$$

where $\lambda_{min}(\boldsymbol{Q})$ is the smallest eigenvalue of $\boldsymbol{Q}$. From the inequality expressed by Eq. (13), we can conclude that whenever $\|\tilde{\boldsymbol{x}}\|$ is outside the region bounded by $\|\tilde{\boldsymbol{x}}\| \leq \Gamma/\lambda_{min}(\boldsymbol{Q})$, $\dot{V} \leq 0$. Thus, according to Barbalat's lemma, $\lim_{t\to\infty} \tilde{\boldsymbol{x}} = 0$, i.e. the estimated state vector converges as $\hat{\boldsymbol{x}} \cong \boldsymbol{x}$.

II.3. THE RADIAL BASIS FUNCTION NEURAL NETWORK (RBFNN)

Consideringthat the USV's functions $f(t, x_2)$ and $g(t)$ are unknown, and hence unavailable for practical implementation of the control system, we need to use and intelligent devices such as RBFNNs to provide approximation of the unknown dynamics. RBFNNs are feedforward networks, made of three layers, namely the input, the hidden and the output layer, which are used to approximate any smooth function on a compact set $\Omega \in \mathbb{R}^n$ using the universal approximation theorem[8, 11].

Two RBFNNs are used in this paper for the approximation of the two unknown USV's functions $f(t, x_2)$ and $g(t)$. The input vectors are selected as$\boldsymbol{x_{e1}} = [\hat{e} \quad \dot{\hat{e}}]^T$with $\hat{e} = \hat{x}_1 - x_{1d}$, and $\boldsymbol{x_{e2}} = [\hat{x}_1 \quad \hat{x}_2]^T$, respectively, for the two RBFNN.With m and n being the numbers of hidden layers, the neural networks' outputs provide approximations of the two functions expressed as follows:

$$\hat{f}\left(\boldsymbol{x_{e1}}|\widehat{\boldsymbol{W}}_{\boldsymbol{1}}\right) = \widehat{\boldsymbol{W}}_1^T\boldsymbol{h}_1(\boldsymbol{x_{e1}}) \tag{14}$$

$$\hat{g}\left(\boldsymbol{x_{e2}}|\widehat{\boldsymbol{W}}_{\boldsymbol{2}}\right) = \widehat{\boldsymbol{W}}_2^T\boldsymbol{h}_2(\boldsymbol{x_{e2}}) \tag{15}$$

where $\widehat{\boldsymbol{W}}_1^T = [W_{11} \quad W_{12} \quad \cdots \quad W_{1m}]$ and $\widehat{\boldsymbol{W}}_2^T = [W_{21} \quad W_{22} \quad \cdots \quad W_{1n}]$ and estimated weighting vectors for which update rules are defined as follows:

$$\dot{\widehat{W}}_1 = \gamma_1^{-1}\hat{s}\boldsymbol{h_1}(\boldsymbol{x_{e1}}) \tag{16}$$

$$\dot{\widehat{W}}_2 = \gamma_2^{-1}\hat{s} \cdot u_i \cdot \boldsymbol{h_2}(\boldsymbol{x_{e2}}) \tag{17}$$

where $\hat{s}$ is a filtered error function defined as follows:

$$\hat{s} = c \cdot \hat{e} + \dot{\hat{e}} \tag{18}$$

with $c > 0$; and $\boldsymbol{h}_1^T(\boldsymbol{x_{e1}}) = [h_{11} \quad h_{12} \quad \cdots \quad h_{1m}]$ and $\boldsymbol{h}_2^T(\boldsymbol{x_{e2}}) = [h_{21} \quad h_{22} \quad \cdots \quad h_{1n}]$ are radial basis vector functions for which the elements are obtained using :

$$h_{1j}(\boldsymbol{x_{e1}}) = \exp\left(-\frac{\|x_{e1}-\boldsymbol{\lambda_{1j}}\|^2}{2\beta_1^2}\right) \tag{19}$$

$$h_{2i}(\boldsymbol{x_{e2}}) = \exp\left(-\frac{\|x_{e2}-\boldsymbol{\lambda_{2j}}\|^2}{2\beta_2^2}\right) \tag{20}$$

with $\lambda_{1j} \in \mathbb{R}^{2\times1}$ and $\lambda_{2j} \in \mathbb{R}^{2\times1}$ being the centric vectors, $\beta_1 \in \mathbb{R}$ and $\beta_2 \in \mathbb{R}$ being the base widths of the radial basis functions, for the two RBFNNs.

The differences between the neural networks' outputs and the exact nonlinear functions they approximate are:

$$\hat{f}(\boldsymbol{x_{e1}}|\widehat{\boldsymbol{W}}_1) - f(t, x_2) = \widetilde{\boldsymbol{W}}_1^T\boldsymbol{h}_1(\boldsymbol{x_{e1}}) - \varepsilon_1(\boldsymbol{x_{e1}}) \tag{21}$$

$$\hat{g}(\boldsymbol{x_{e2}}|\widehat{\boldsymbol{W}}_2) - g(t) = \widetilde{\boldsymbol{W}}_2^T\boldsymbol{h}_2(\boldsymbol{x_{e2}}) - \varepsilon_2(\boldsymbol{x_{e2}}) \tag{22}$$

where $\widetilde{\boldsymbol{W}}_1$ and $\widetilde{\boldsymbol{W}}_2$ are errors on the approximated weighting vectors; $\varepsilon_1(\boldsymbol{x_{e1}})$ and $\varepsilon_2(\boldsymbol{x_{e2}})$ are the neural networks' approximation errors.

Assumption: For each of the two RBFNNs, there exist an unknown constant E_k, $k = 1,2$, which is the upper bound of the approximation errors $\varepsilon_k(\boldsymbol{x_{ek}})$ over the compact set $\Omega \in \mathbb{R}^2$, i.e. $\max_{x_{ek}}|\varepsilon_k(\boldsymbol{x_{ek}})| \leq \mathrm{E}_k$.

III. FAULT-TOLERANT NONLINEAR CONTROLLER DESIGN

Considering a particular situation where full state measurement is unavailable, system's dynamics are uncertain, the system may be subject to external disturbances and actuation faults, a control law that can suppress the adverse effects of these perturbations is needed. Therefore, for tackling these challenges, we propose as control law expressed as follows, for the actuator's input:

$$u_i = -\frac{1}{\hat{g}(x_{e2}|\widehat{\boldsymbol{W}}_2)}\left[c\dot{\hat{e}} - \ddot{x}_{1d} + \hat{f}(\boldsymbol{x_{e1}}|\widehat{\boldsymbol{W}}_1) + \hat{\eta}(t)T(\hat{s}) + K_1E(\hat{s})\right] \tag{23}$$

with $\hat{e} = \hat{x}_1 - x_{1d}$,$\hat{s} = c \cdot \hat{e} + \dot{\hat{e}}$, $T(\hat{s}) = (\exp(4\hat{s}) - 1)/(\exp(4\hat{s}) + 1)$, $E(\hat{s}) = \hat{s}/(\exp(\hat{s}) + 1)$.
$\hat{\eta}(t)$ is a time varying parameter for which the value is adaptive online to tackle effects related to unknown external disturbances, actuator's fault and RBFNNs approximation errors. This parameter is computed using:

$$\hat{\eta}(t) = \hat{\eta}_1(t) + \eta_2(t) \tag{24}$$

where

$$\dot{\hat{\eta}}_1(t) = |\hat{s}|/\gamma_\eta \tag{25}$$

and

$$\eta_2(t) = \rho(|\hat{\varepsilon}_1| + u_{max} \cdot |\hat{\varepsilon}_2|) \tag{26}$$

where $\rho > 1$ is an arbitrary design parameter;$\hat{\varepsilon}_1$ and $\hat{\varepsilon}_2$ are estimates values of RBFNNs approximation errors, which can be obtained from:

$$\dot{\hat{\varepsilon}}_1(t) = \hat{s}/\gamma_{\varepsilon_1} \tag{27}$$

$$\dot{\hat{\varepsilon}}_2(t) = \hat{s} \cdot u_i/\gamma_{\varepsilon_2} \tag{28}$$

Theorem 1: Considering the good convergence property of the high-gain state observer, demonstrated by Eq. (13), the control law expressed by Eqs. (23)-(28), and constrained by Eq. (9), guarantees that all signals in the closed-loop system remain bounded and the tracking error $e(t)$ or $\hat{e}(t)$ converges asymptotically towards zero.

In order to provide proof to this theorem, let us define the following candidate Lyapunov's function:

$$V = V_1 + V_2 \tag{29}$$

where

$$V_1 = \frac{1}{2}s^2 + \frac{1}{2}\gamma_1 \widetilde{W}_1^T \widetilde{W}_1 \; + \frac{1}{2}\gamma_2 \widetilde{W}_2^T \widetilde{W}_2 \tag{30}$$

and

$$V_2 = \frac{1}{2}\gamma_\eta \tilde{\eta}_1^2 + \frac{1}{2}\gamma_{\varepsilon_1}\tilde{\varepsilon}_1^2 + \frac{1}{2}\gamma_{\varepsilon_2}\tilde{\varepsilon}_2^2 \tag{31}$$

where $\gamma_1 > 0$, $\gamma_2 > 0$, $\gamma_\eta > 0$, $\gamma_{\varepsilon_1} > 0$, and $\gamma_{\varepsilon_2} > 0$ are the learning rates for $\widehat{W}_1\ (t)$, $\widehat{W}_2\ (t)$, $\hat{\eta}_1\ (t)$, $\hat{\varepsilon}_1\ (t)$ and $\hat{\varepsilon}_1\ (t)$, respectively. Errors on $\widehat{W}_1\ (t)$, $\widehat{W}_2\ (t)$, $\hat{\eta}_1\ (t)$, $\hat{\varepsilon}_1\ (t)$ and $\hat{\varepsilon}_1\ (t)$, are defined as follows:

$$\widetilde{W}_1\ (t) = \widehat{W}_1\ (t) - W_1^* \tag{32}$$
$$\widetilde{W}_2\ (t) = \widehat{W}_2\ (t) - W_2^* \tag{33}$$
$$\tilde{\eta}_1\ (t) = \hat{\eta}_1\ (t) - \eta_1^* \tag{34}$$
$$\tilde{\varepsilon}_1\ (t) = \hat{\varepsilon}_1\ (t) - \varepsilon_1(\boldsymbol{x_{e1}}) \tag{35}$$
$$\tilde{\varepsilon}_2\ (t) = \hat{\varepsilon}_2\ (t) - \varepsilon_2(\boldsymbol{x_{e2}}) \tag{36}$$

where W_1^*,$W_2^*$and $\eta_1^* \gg D(t,u_i)$are unknown optimal parameter values used here only for analytic purpose.

By performing the first-time derivative of Eq. (30) we obtain:

$$\dot{V}_1 = s\dot{s} + \gamma_1 \widetilde{W}_1^T \dot{\widetilde{W}}_1 \; + \gamma_2 \widetilde{W}_2^T \dot{\widetilde{W}}_2 \tag{37}$$

With $s = ce + \dot{e}$, where $e = x_1 - x_{1d}$, and with $e \cong \hat{e}$, the fist-time derivative of s is obtained, using Eqs. (5),(21)-(23), as follows:

$$\begin{aligned} \dot{s} &= c\dot{e} - \ddot{x}_{1d} + f\ \ (t,x_2) + \left[g(t) - \hat{g}\left(\boldsymbol{x_{e2}}|\widehat{\boldsymbol{W}}_2\right)\right]u_i + D(t,u_i) + \hat{g}\left(\boldsymbol{x_{e2}}|\widehat{\boldsymbol{W}}_2\right)u_i \\ &= \left[f\ \ (t,x_2) - \hat{f}\left(\boldsymbol{x_{e1}}|\widehat{\boldsymbol{W}}_1\right)\right] + \left[g(t) - \hat{g}\left(\boldsymbol{x_{e2}}|\widehat{\boldsymbol{W}}_2\right)\right]u_i + c\left(\dot{e} - \dot{\hat{e}}\right) + D(t,u_i) - \hat{\eta}(t)T(\hat{s}) - K_1E(\hat{s}) \\ &= \left[\varepsilon_1(\boldsymbol{x_{e1}}) - \widetilde{\boldsymbol{W}}_1^T\boldsymbol{h}_1(\boldsymbol{x_{e1}})\right] + \left[\varepsilon_2(\boldsymbol{x_{e2}}) - \widetilde{\boldsymbol{W}}_2^T\boldsymbol{h}_2(\boldsymbol{x_{e2}})\right]u_i + D(t,u_i) - \hat{\eta}(t)T(\hat{s}) - K_1E(\hat{s}) \end{aligned} \tag{38}$$

By applying Eq. (38) in Eq. (37), where Eqs. (16), (17), (32) and (33) are used,and considering that thanks to the observer's convergence $s \cong \hat{s}$,we obtain:

$$\begin{aligned} \dot{V}_1 &= \widetilde{\boldsymbol{W}}_1^T\left(\gamma_1\dot{\widetilde{W}}_1 \; - s\boldsymbol{h}_1(\boldsymbol{x_{e1}})\right) + \widetilde{\boldsymbol{W}}_2^T\left(\gamma_2\dot{\widetilde{W}}_2 \; - s\boldsymbol{h}_2(\boldsymbol{x_{e2}})u_i\right) + s\varepsilon_1(\boldsymbol{x_{e1}}) + s\varepsilon_2(\boldsymbol{x_{e2}})u_i + sD(t,u_i) - s\hat{\eta}(t)T(\hat{s}) - sK_1E(\hat{s}) \\ &= \widetilde{\boldsymbol{W}}_1^T\boldsymbol{h}_1(\boldsymbol{x_{e1}})(s - \hat{s}) + \widetilde{\boldsymbol{W}}_2^T\boldsymbol{h}_2(\boldsymbol{x_{e2}})(s - \hat{s}) + s\varepsilon_1(\boldsymbol{x_{e1}}) + s\varepsilon_2(\boldsymbol{x_{e2}})u_i + sD(t,u_i) - s\hat{\eta}(t)T(\hat{s}) - sK_1E(\hat{s}) \\ &= s\varepsilon_1(\boldsymbol{x_{e1}}) + s\varepsilon_2(\boldsymbol{x_{e2}})u_i + sD(t,u_i) - s\hat{\eta}(t)T(\hat{s}) - sK_1E(\hat{s}) \end{aligned} \tag{39}$$

The first-time derivative of Eq. (31); where Eqs. (34)-(36) are used,gives:

$$\dot{V}_2 = \gamma_\eta\tilde{\eta}_1\ \dot{\tilde{\eta}}_1 + \gamma_{\varepsilon_1}\tilde{\varepsilon}_1\ \dot{\tilde{\varepsilon}}_1 + \gamma_{\varepsilon_2}\tilde{\varepsilon}_2\ \dot{\tilde{\varepsilon}}_2 = \gamma_\eta\tilde{\eta}_1\ \dot{\hat{\eta}}_1 + \gamma_{\varepsilon_1}\tilde{\varepsilon}_1\ \dot{\hat{\varepsilon}}_1 + \gamma_{\varepsilon_2}\tilde{\varepsilon}_2\ \dot{\hat{\varepsilon}}_2 \tag{40}$$

Using Eqs. (39) and (40), the first-time derivative of Eq. (29), where Eqs. (27), (28), (35) and (36) are used, with $s \cong \hat{s}$ gives:

$$\begin{aligned} \dot{V} &= s\varepsilon_1(\boldsymbol{x_{e1}}) + s\varepsilon_2(\boldsymbol{x_{e2}})u_i + sD(t,u_i) - s\hat{\eta}(t)T(\hat{s}) - sK_1E(\hat{s}) + \gamma_\eta\tilde{\eta}_1\ \dot{\hat{\eta}}_1 + \gamma_{\varepsilon_1}\tilde{\varepsilon}_1\ \dot{\hat{\varepsilon}}_1 + \gamma_{\varepsilon_2}\tilde{\varepsilon}_2\ \dot{\hat{\varepsilon}}_2 \\ &= s\left(\hat{\varepsilon}_1(\boldsymbol{x_{e1}}) - \tilde{\varepsilon}_1(\boldsymbol{x_{e1}})\right) + su_i\left(\hat{\varepsilon}_2(\boldsymbol{x_{e2}}) - \tilde{\varepsilon}_2(\boldsymbol{x_{e2}})\right) + sD(t,u_i) - s\hat{\eta}(t)T(\hat{s}) - sK_1E(\hat{s}) + \gamma_\eta\tilde{\eta}_1\ \dot{\hat{\eta}}_1 + \gamma_{\varepsilon_1}\tilde{\varepsilon}_1\ \dot{\hat{\varepsilon}}_1 + \gamma_{\varepsilon_2}\tilde{\varepsilon}_2\ \dot{\hat{\varepsilon}}_2 \\ &= \tilde{\varepsilon}_1(\boldsymbol{x_{e1}})\left(\gamma_{\varepsilon_1}\dot{\hat{\varepsilon}}_1 - s\right) + \tilde{\varepsilon}_2(\boldsymbol{x_{e2}})\left(\gamma_{\varepsilon_2}\dot{\hat{\varepsilon}}_2 - su_i\right) + sD(t,u_i) - s\hat{\eta}(t)T(\hat{s}) - sK_1E(\hat{s}) + \gamma_\eta\tilde{\eta}_1\ \dot{\hat{\eta}}_1 + s\hat{\varepsilon}_1(\boldsymbol{x_{e1}}) + su_i\hat{\varepsilon}_2(\boldsymbol{x_{e2}}) \\ &= \tilde{\varepsilon}_1(\boldsymbol{x_{e1}})(\hat{s} - s) + \tilde{\varepsilon}_2(\boldsymbol{x_{e2}})u_i(\hat{s} - s) + sD(t,u_i) - s\hat{\eta}(t)T(\hat{s}) - sK_1E(\hat{s}) + \gamma_\eta\tilde{\eta}_1\ \dot{\hat{\eta}}_1 + s\hat{\varepsilon}_1(\boldsymbol{x_{e1}}) + su_i\hat{\varepsilon}_2(\boldsymbol{x_{e2}}) \\ &= sD(t,u_i) - s\hat{\eta}(t)T(\hat{s}) - K_1\frac{s\hat{s}}{\exp(\hat{s})+1} + \gamma_\eta\tilde{\eta}_1\ \dot{\hat{\eta}}_1 + s\hat{\varepsilon}_1(\boldsymbol{x_{e1}}) + su_i\hat{\varepsilon}_2(\boldsymbol{x_{e2}}) \\ &\le s\Delta - s\hat{\eta}(t)T(\hat{s}) - K_1\frac{\hat{s}^2}{\exp(\hat{s}) + 1} + \gamma_\eta\tilde{\eta}_1\ \dot{\hat{\eta}}_1 + |s||\hat{\varepsilon}_1(\boldsymbol{x_{e1}})| + |s|u_{max}|\hat{\varepsilon}_2(\boldsymbol{x_{e2}})| \end{aligned} \tag{41}$$

Considering that, in case of perturbations, we may have $|\hat{s}| \gg 0$ and $|T(\hat{s}) = (\exp(4\hat{s}) - 1)/(\exp(4\hat{s}) + 1)| \cong 1$ such that Eq. (42), where Eqs. (24)-(26) are used, becomes:

| e-ISSN: 2278 – 8875, p-ISSN: 2320 – 3765| www.ijareeie.com | Impact Factor: 7.122|

|| Volume 9, Issue 7, July 2020 ||

$$\dot{V} \leq s\Delta - s\big(\hat{\eta}_1(t) + \eta_2(t)\big) - K_1 \frac{\hat{s}^2}{\exp(\hat{s}) + 1} + \gamma_\eta \tilde{\eta}_1 \, \dot{\hat{\eta}}_1 + |s||\hat{\varepsilon}_1(\boldsymbol{x_{e1}})| + |s|u_{max}|\hat{\varepsilon}_2(\boldsymbol{x_{e2}})| + \eta_1^* s - \eta_1^* s$$

$$\leq |s|\big(|\hat{\varepsilon}_1(\boldsymbol{x_{e1}})| + u_{max}|\hat{\varepsilon}_2(\boldsymbol{x_{e2}})| - \eta_2(t)\big) + s\Delta + |s|(-\hat{\eta}_1(t) + \eta_1^*) - K_1 \frac{\hat{s}^2}{\exp(\hat{s})+1} + \gamma_\eta \tilde{\eta}_1 \, \dot{\hat{\eta}}_1 - \eta_1^* s \quad (42)$$

$$= |s|\big(|\hat{\varepsilon}_1(\boldsymbol{x_{e1}})| + u_{max}|\hat{\varepsilon}_2(\boldsymbol{x_{e2}})| - \eta_2(t)\big) + s\Delta - K_1 \frac{\hat{s}^2}{\exp(\hat{s}) + 1} + \tilde{\eta}_1 \left(\gamma_\eta \dot{\hat{\eta}}_1 - |s|\right) - \eta_1^* s$$

$$= |s|\big(|\hat{\varepsilon}_1(\boldsymbol{x_{e1}})| + u_{max}|\hat{\varepsilon}_2(\boldsymbol{x_{e2}})| - \eta_2(t)\big) + s\Delta - K_1 \frac{\hat{s}^2}{\exp(\hat{s}) + 1} - \eta_1^* s$$

$$\leq |s|\left(\frac{1}{\rho} - 1\right)\eta_2(t) + |s|(\Delta - \eta_1^*) - K_1 \frac{\hat{s}^2}{\exp(\hat{s}) + 1}$$

with $\rho > 1$, $K_1 > 0$ and $\eta_1^* > \Delta$, one can notice that $\dot{V} \leq 0$. Therefore, with the proposed observed and RBFNN based control law, the USV's steering closed-loop system is asymptotically stable despite potential perturbations related to the occurrence of parameter changes, external disturbance and actuation faults. Hence, the USV can successfully achieve its mission in adverse conditions, as according to the Barbalat's lemma, the tracking error $e \to 0$ when $t \to \infty$.

IV. SIMULATION RESULTS AND DISCUSSIONS

In order to illustrate the efficiency of the proposed autopilot for the DH-01 USV, let us perform a MATLAB/SIMULINK simulation of the control system with an unavailable yaw rate measurement, unknown external disturbance, actuation loss of efficiency and parameter changes. The specifications of the vehicle are as follows [8, 14, 19]: length of 110cm, width of 36cm, weight of 5.4kg and max power of 36W.

The parameters used for the RBFNNs are selected as: $m = n = 5$, $\lambda_{1j} = \lambda_{2j} = [0.10 \quad 0.10]^T$, and $\beta_1 = \beta_2 = 0.5$. The parameters for the high-gain observer are chosen as follows: $k_1 = 5$, $k_2 = 7$ and $\epsilon = 5.5 \times 10^{-2}$. The other controller's parameters are selected as follows: $c = 5$, $K_1 = 2$, $\gamma_\eta = 0.35$, $\gamma_{\varepsilon_1} = \gamma_{\varepsilon_2} = 5$, $\gamma_1 = 0.09$ and $\gamma_2 = 15$. Considering physical limitations of the actuator or saturation, the control is restricted between $-35°$ $(-0.61\,rad)$ and $35°$ $(0.61\,rad)$.

In order to illustrate the advantages of the controller proposed in this paper, its results are compared with those obtained using itsSMC used in [8] with all state variables available.The SMC is known for its robustness with regards to some perturbations. We consider the same simulation scenario as in [8].Let us consider that the reference yaw angle is $\psi_d(t) = 0.5\sin(0.2t)$ and that the external disturbance is $d(t) = 0.2\sin(t)$. We consider that for $t < 10sec$ the vessel has a cruise speed of $7\,knots$ (12.964km/h), speed for which the DH-01 parameters are as follows [8, 19]: $K(t) = 0.366$, $T(t) = 0.24$, $\alpha(t) = 0.35$, and $\beta(t) = 0.3$. For $t \geq 10$, we consider that the ship's parameters become$K(t) = 0.266$, $T(t) = 0.29$, $\alpha(t) = 0.4$, and $\beta(t) = 0.35$. For studying the behaviour of the control system, we consider that from $t \geq 20$ the actuator looses 50% of its effectiveness.

The results of this simulation are depicted in Figs. 2 to 4. Figure 2(a) represents the desired yaw angle value $\psi_d(t)$ along with the USV's yaw angle $\psi\ \ (t)$ obtained using the controller proposed in this paper, the yaw angle estimate $\psi_a(t)$ provided by the state observer and the yaw angle $\psi_{smc}(t)$ obtained using the traditional SMC. As one can observe from this figure, the proposed controller provides better tracking results in different operating conditions. This can be better observed in Fig. 2(b) where the tracking error on the yaw angle is represented, and where it is obvious that the tracking error is smaller with the proposed controller in all situations. One can see clearly that at $t \geq 10sec$, when the USV parameters vary and particularly when the actuation fault occurs at $t = 20sec$, an important increase of the yaw error happens in case the SMC is applied. However, with the proposed adaptive fault-tolerant controller, this error on the yaw angle does not change much and remains restricted in small boundaries despite the occurrence of the disturbances and the use of a state observer. This superiority of the proposed controller is more obvious in Fig. 3(b) where one can see that with the SMC the error on yaw rate is far bigger. It is worth reminding that the proposed controller uses observed states, unlike the traditional SMC. Figure 4 depicts the rudder angle provided by the proposed controller and the SMC, respectively. One can observe that the two control signals are not too different even though they yield some very different results.

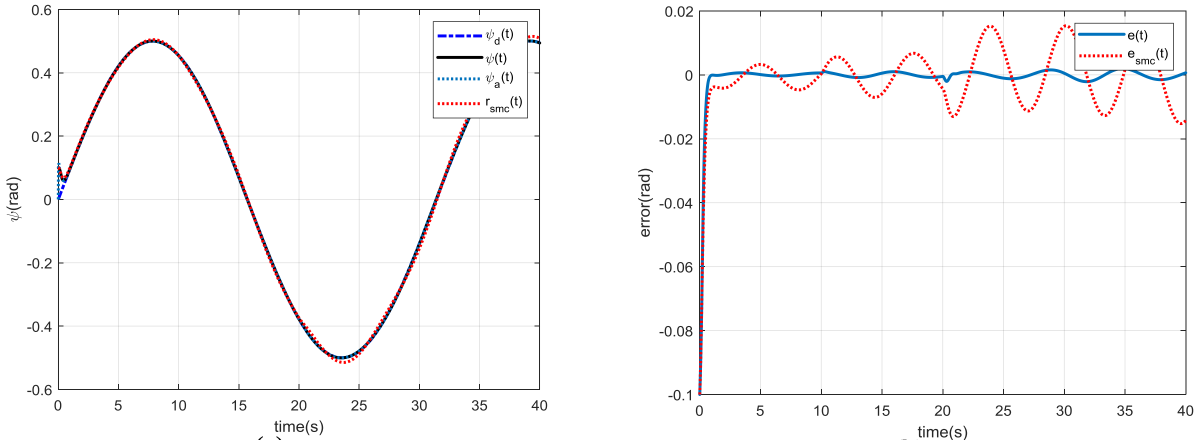

(a) (b)

Figure 2. (a) Desired yaw angle $\psi_d(t)$ compared with the output obtained using the traditional SMC and the proposed controller. (b) Tracking error of the yaw angle obtained with each controller

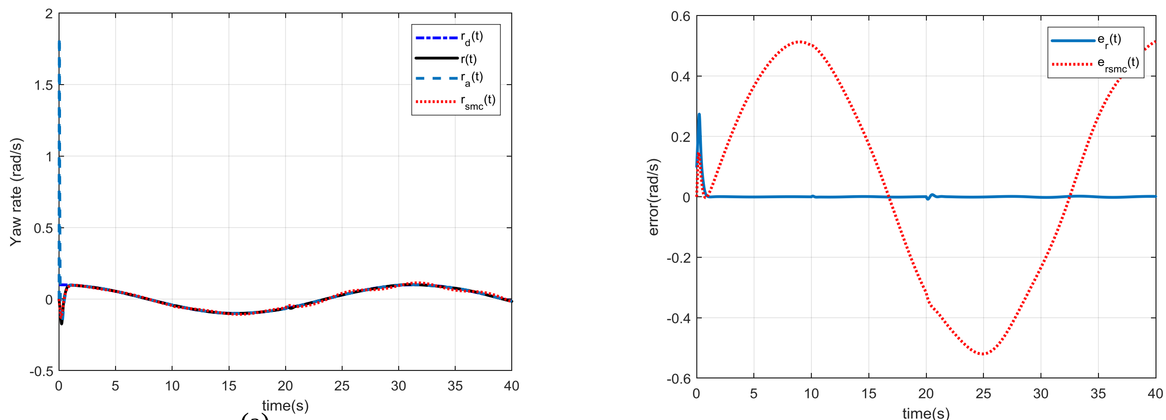

(a) (b)

Figure 3. (a) Desired yaw rate $r_d(t)$ compared with the yaw rate obtained using the traditional SMC and the proposed controller. (b) Tracking error of the yaw rate obtained with each controller

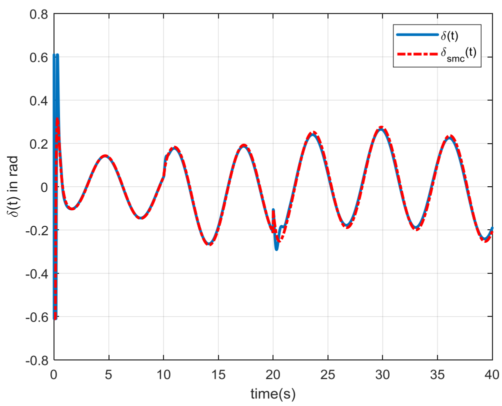

Figure 4. Control actions $u(t) = \delta(t)$ obtained with the proposed controller and with the SMC

IV. SIMULATION RESULTS AND DISCUSSIONS

The control problem of an Unmanned Surface Vehicle steering system subject to unknown dynamics, external disturbances caused by the ship's operating conditions and environment, actuation failure and unavailable state measurement have been addressed in this paper. Using Radial Basis Functions Neural Networks, a high-gain state observer and some dynamic parameters, an adaptive nonlinear controller has been developed such that all the aforementioned challenges have been tackled simultaneously. Using the Lyapunov's theory, a stability analysis has been performed. A DH-01 USV has been simulated on MATLAB/SIMULINK, with the proposed autopilot, which has been proved to be very efficient in terms of tracking accuracy, in different operating conditions. These good results have been put in display by their comparison with those obtained using the traditional sliding mode control, which is known for its robustness. Hence, thanks to the proposed controller the vessel can perform its missions autonomously and successfully despite some adverse conditions.

REFERENCES

[1] M. N. Azzeria, F. A. Adnanb and M. Z. M. Zaina, "Review of Course Keeping Control System for Unmanned Surface Vehicle," Jurnal teknologi, vol. 74, no. 5, pp. 11-20, 2015.
[2] L. Chengxing, Y. Haisheng, H. Zhili, L. Lei and C. Jieru, "Speed and Heading Control of an Unmanned Surface Vehicle Based on State Error PCH Principle," Hindawi Mathematical Problems in Engineering, vol. 2018, p. 9, 2018.
[3] A. M. Waleed, A. N. Ahmed, A. Y. Majid, S. Ashraf and A. M. Ahmed, "Design and Implementation of an Unmanned Surface Vehicle for Oil Spill Handling," in Proceedings of the 1st International Conference on Unmanned Vehicle Systems (UVS), Muscat, Oman, 2019.
[4] Z. X. Liu, C. Yuan and Y. Zhang, "Linear Parameter Varying Adaptive Control of an Unmanned Surface Vehicle," IFAC-PapersOnLine, vol. 2015, pp. 140-145, 2015.
[5] C. Massimo, B. Marco and B. •. Riccardo, "Basic navigation, guidance and control of an Unmanned Surface Vehicle," Auton Robot , vol. 25, p. 349–365, 2008.
[6] T. Ngoc-Huy, C. Hyeung-Sik, B. Se-Hoon and S. Hee-Young, "Tracking Control of an Unmanned Surface Vehicle," in AETA 2013: Recent Advances in Electrical Engineering and Related Sciences, Berlin, Springer, 2013, pp. 575-584.
[7] B. Yiming, Z. Yongsheng and Y. F. , "The Unmanned Surface Vehicle Course Tracking Control with Input Saturation," in Proceedings of the 36th Chinese Control Conference, Dalian, 2017.
[8] W. Lili, S. Yixin, Z. Huajun, T. Yongchuan and S. Binghua, "Neural adaptive sliding mode controller for unmanned surface vehicle steering system," Advances in mechanical engineering, vol. 10, no. 9, pp. 1-12, 2018.
[9] M. Faramin, R. Goudarzi and A. Maleki, "Track-keeping observer-based robust adaptive control of an unmanned surface vessel by applying a 4-DOF maneuvering model," Ocean Engineering, vol. 183, pp. 11-23, 2019.
[10] Z. Pengchao, "Dynamic Surface Adaptive Robust Control of Unmanned Marine Vehicles with Disturbance Observer," Hindawi Journal of Robotics, vol. 2018, p. 6, 2018.
[11] M. Dongdong, W. Guofeng, F. Yunsheng, B. Yiming and Z. Yongsheng, "Fuzzy-Based Optimal Adaptive Line-of-Sight Path Following for Underactuated Unmanned Surface Vehicle with Uncertainties and Time-Varying Disturbances," Hindawi Mathematical Problems in Engineering, vol. 2018, p. 12, 2018.
[12] H. Zhijian, L. Xinze, W. Jiayi, Z. Guichen and L. Yihua, "Adaptive Navigating Control Based on the Parallel Action-Network ADHDP Method for Unmanned Surface Vessel," Hindawi Advances in Materials Science and Engineering, vol. 2019, p. 8, 2019.
[13] R. Sutton, S. Sharma and T. Xao, "Adaptive navigation systems for an unmanned surface vehicle," Journal of Marine Engineering & Technology, vol. 10, no. 3, p. 19, 2014.
[14] P. Zhouhua, T. Yong, W. Dan and L. Lu, "Autopilot Design for a Robotic Unmanned Surface Vehicle," in Proceedings of the 34th Chinese Control Conference, Hangzou, 2015.
[15] J. Quanquan, L. Ye, L. Yulei, M. Yugang, J. Wen and W. Haowei, "Information fusion model-free adaptive control algorithm and unmanned surface vehicle heading control," Applied Ocean Research, vol. 90, p. 7, 2019.
[16] A. S. K. Annamalai, R. Sutton and C. Yang, "Robust Adaptive Control of an Uninhabited Surface Vehicle," J Intell Robot Syst, p. 20, 2014.
[17] W. Lili, Z. Chun and C. Yan, "Adaptive steering control system of the USV with friction compensation," in 2018 Chinese Automation Congress (CAC), Xi'an, 2018.
[18] T. Fossen, Handbook of marine craft hydrodynamics and motion control, Chichester: John Wiley and Sons Ltd, 2011.
[19] Z. Peng, D. Wang, W. Wang and L. Liu, "Neural adaptive steering of an unmanned surface vehicle with measurement," Neural adaptive steering of an unmanned surface vehicle with measurement noises, vol. 186, pp. 228-234, 2016.
[20] J. H. Richter, Reconfigurable Control of Nonlinear Dynamical Systems, Berlin: Springer-Verlag Berlin Heidelberg, 2011.
[21] B. Mushage, J. Chedjou and K. Kyamakya, "Observer-based fuzzy adaptive fault-tolerant nonlinear control for uncertain strict-feedback nonlinear systems with unknown control direction and its applications," Nonlinear Dyn.
[22] N. Goléa, A. Goléa, K. Barra and T. Bouktir, "Observerbased adaptive control of robot manipulators: fuzzy systems approach," Appl. Soft Comput, vol. 22, pp. 563-574, 2014.
[23] K. Veluvolu, M. Kim and D. Lee, " Nonlinear sliding mode high-gain observers for fault estimation," Int. J. Syst. Sci. , vol. 42, pp. 1065-1074, 2011.